

The chemistry of a CCl₂F₂ radio frequency discharge

Citation for published version (APA):

Stoffels, W. W., Stoffels - Adamowicz, E., Haverlag, M., Kroesen, G. M. W., & Hoog, de, F. J. (1995). The chemistry of a CCl₂F₂ radio frequency discharge. *Journal of Vacuum Science and Technology A*, 13(4), 2058-2066. <https://doi.org/10.1116/1.579652>

DOI:

[10.1116/1.579652](https://doi.org/10.1116/1.579652)

Document status and date:

Published: 01/01/1995

Document Version:

Publisher's PDF, also known as Version of Record (includes final page, issue and volume numbers)

Please check the document version of this publication:

- A submitted manuscript is the version of the article upon submission and before peer-review. There can be important differences between the submitted version and the official published version of record. People interested in the research are advised to contact the author for the final version of the publication, or visit the DOI to the publisher's website.
- The final author version and the galley proof are versions of the publication after peer review.
- The final published version features the final layout of the paper including the volume, issue and page numbers.

[Link to publication](#)

General rights

Copyright and moral rights for the publications made accessible in the public portal are retained by the authors and/or other copyright owners and it is a condition of accessing publications that users recognise and abide by the legal requirements associated with these rights.

- Users may download and print one copy of any publication from the public portal for the purpose of private study or research.
- You may not further distribute the material or use it for any profit-making activity or commercial gain
- You may freely distribute the URL identifying the publication in the public portal.

If the publication is distributed under the terms of Article 25fa of the Dutch Copyright Act, indicated by the "Taverne" license above, please follow below link for the End User Agreement:

www.tue.nl/taverne

Take down policy

If you believe that this document breaches copyright please contact us at:

openaccess@tue.nl

providing details and we will investigate your claim.

The chemistry of a CCl_2F_2 radio frequency discharge

W. W. Stoffels, E. Stoffels, M. Haverlag, G. M. W. Kroesen, and F. J. de Hoog
Department of Physics, Eindhoven University of Technology, 5600 MB Eindhoven, The Netherlands

(Received 24 October 1994; accepted 11 February 1995)

A systematic study of the chemistry of stable molecules and radicals in a low pressure CCl_2F_2 radio frequency discharge for dry Si etching has been performed. Various particle densities have been measured and modeled. The electron density, needed as an input parameter to model the CCl_2F_2 dissociation, is measured by a microwave cavity method. The densities of stable molecules, like CClF_3 , CF_4 , $1,2\text{-C}_2\text{Cl}_2\text{F}_4$ and the etch product SiF_4 , are measured by Fourier transform absorption spectroscopy. The density of the CF_2 radical is measured by means of absorption spectroscopy with a tunable diode laser. Its density is in the order of 10^{19} m^{-3} . All density measurements are presented as a function of various plasma parameters. Moreover, optical emission intensities of Cl and F have been recorded as a function of plasma parameters. It appears that the feed gas (CCl_2F_2) is substantially dissociated (about 70%–90%) in the discharge. Based on the obtained data the dissociation rates of several molecules have been estimated. The measured total dissociation rate of CCl_2F_2 is $8 \times 10^{-15} \text{ m}^3 \text{ s}^{-1}$. For this molecule the dissociation rate is substantially higher than the dissociative attachment rate ($10^{-15} \text{ m}^3 \text{ s}^{-1}$). The dissociation rate for CClF_3 is $2 \times 10^{-15} \text{ m}^3 \text{ s}^{-1}$ and for CF_4 about $3 \times 10^{-16} \text{ m}^3 \text{ s}^{-1}$. The total dissociation rate of $\text{C}_2\text{Cl}_2\text{F}_4$ is higher than $5 \times 10^{-15} \text{ m}^3 \text{ s}^{-1}$, of which $2.5 \pm 0.5 \times 10^{-15} \text{ m}^3 \text{ s}^{-1}$ is due to dissociative attachment. Furthermore it has been found that the presence of a silicon wafer strongly affects the plasma chemistry. Optical emission measurements show that the densities of halogen radicals are significantly depleted in presence of Si. Moreover, the densities of several halocarbon molecules display a negative correlation with the density of the etch product SiF_4 . © 1995 American Vacuum Society.

I. INTRODUCTION

The widespread use of radio frequency (rf) plasmas for industrial surface modification requires a detailed study of the chemical nature of the active process gases under discharge conditions. The large variety of chemical reactions in the gas phase and at the surface together with uncertainties in the cross sections for these processes make it necessary to verify all modeling approaches experimentally. The obtained experimental data on the particle densities and reaction rates can remove some of those ambiguous points if used to test the numerical models. In this article the chemistry of CCl_2F_2 , including stable molecules, radicals, and their behavior under various plasma conditions, is treated. CCl_2F_2 is extremely efficient as an etchant and it is commonly used for the reactive ion etching of silicon, germanium and silicon oxide.¹ The mixtures of CCl_2F_2 with argon are especially useful, as they combine the chemical reactivity of a molecular gas with the physical sputtering efficiency of argon. These mixtures also attract much attention due to the formation of macroscopic clusters during the etching process.^{2,3} Elimination of the unwanted dust contamination can be realized only by a good understanding of the discharge chemistry.

A typical feature of a low pressure (5–500 mTorr) rf discharge is that its electron temperature (2–3 eV)⁴ is much higher than the heavy particle temperature, which does not differ much from room temperature.⁵ The electron density is typically 10^{15} m^{-3} . In this work we show that even in this low pressure weakly ionized plasma efficient dissociation and conversion of the feed gas take place. The rate constants for these processes are essential in modeling discharge chem-

istry. However, there is no literature data on the total electron induced dissociation rate of CCl_2F_2 and related halocarbon molecules. Therefore we have developed a simple model, allowing the determination of these magnitudes by fitting the measured molecule densities and their dependencies upon plasma parameters. The electron density, needed as an input parameter for this model, is measured for all plasma conditions of interest. The details of this procedure together with possible mechanisms for CCl_2F_2 dissociation are discussed in Sec. II. Furthermore, a comparison is made between etching conditions (in presence of a silicon wafer on the electrode) and a “pure” CCl_2F_2 plasma, without the Si substrate. The presence of a wafer appears to have a large influence on the plasma composition. Surface or plasma reactions of halogen radicals with silicon result in a drastic reduction of their densities; at the same time, etch products appear in the plasma.

II. REACTIONS

Even though CCl_2F_2 is relatively inert in the gas phase, it breaks up readily in the plasma to form a wide variety of new species. As the C–F bond is stronger than the C–Cl bond (4.8 eV and 3.3 eV, respectively), the dominant radicals and positive ions formed from CCl_2F_2 are relatively fluorine rich. The most abundant halocarbon radicals are expected to be CClF_2 and CF_2 . As the former has an unpaired electron, it is expected to be reactive in the gas phase as well as at the surface. The latter one (CF_2) is relatively stable. Eventually, stable molecules like $\text{C}_2\text{Cl}_2\text{F}_4$, CClF_3 and CF_4 are formed as a result of radical recombination. The densities of chlorine rich species (CCl_4 , CCl_3F) are expected to be relatively low,

as their production from CCl_2F_2 requires replacing of a strong C–F bond by a weaker one. Moreover, once formed, these molecules are very quickly destroyed by dissociative electron attachment. The absence of highly chlorinated species in the plasma has been experimentally verified by O'Neill *et al.*⁶ Chlorine stripped from the halocarbon molecules is expected to form large amounts of Cl_2 . In the presence of a silicon wafer various etch products are present in the plasma. In analogy to halocarbons, the fluorine rich silicon halides are expected to be most abundant.

The total dissociation rate of CCl_2F_2 by electrons is not known. However, this magnitude (k_{dis}) can be determined from the measured dissociation degree of CCl_2F_2 in the plasma if the electron density (n_e) is known. Let us consider the following production/destruction balance:

$$k_{\text{dis}}n_en_{\text{CCl}_2\text{F}_2} + \nu_{\mathcal{F}}n_{\text{CCl}_2\text{F}_2} = \nu_{\mathcal{F}}n_{\text{total}} + \nu_{\text{ass}}(n_{\text{total}} - n_{\text{CCl}_2\text{F}_2}), \quad (1)$$

where $\nu_{\mathcal{F}}$ is the reciprocal of the residence time of particles in the plasma volume. For our plasma volume (0.6 dm^3 for the open configuration) $\nu_{\mathcal{F}} = 21 \times \mathcal{F}/p$, where the flow rate \mathcal{F} is given in sccm and the pressure p in mTorr. Here n_{total} denotes the total gas density, obtained from pressure, and ν_{ass} the association frequency (the formation of CCl_2F_2 from other molecules). Equation (1) can be rewritten in the following form:

$$\frac{n_{\text{CCl}_2\text{F}_2}}{n_{\text{total}}} = \frac{\nu_{\mathcal{F}} + \nu_{\text{ass}}}{k_{\text{dis}}n_e + \nu_{\mathcal{F}} + \nu_{\text{ass}}}. \quad (2)$$

Equation (2) has been used to fit the experimental data. The association frequency ν_{ass} , which in this case is a minor correction, is estimated by extrapolating the CCl_2F_2 fraction to $\mathcal{F} = 0$.

It can be assumed that, in a low pressure discharge with cold heavy particles, the gas phase loss of stable molecules is due to electron induced reactions. Possible mechanisms of breaking up a molecular bond by electrons are electron impact dissociation and dissociative electron attachment. Also, ionization of a molecule can be followed by breaking one or more bonds. This is particularly true for halocarbon molecules, as their parent ions are unstable and therefore always dissociate. Cross sections for ionization and attachment are given by Pejcev *et al.*⁷ Dissociative attachment can play an important role in a low temperature plasma, as it requires less electron energy than the “normal” dissociation. The exact contribution of ionization is difficult to estimate, as this process is strongly dependent on the electron temperature and energy distribution. However, it is typically slower than electron impact dissociation.⁸ It is interesting to estimate to what extent dissociative attachment contributes to the breaking up of CCl_2F_2 . For highly chlorinated molecules like CCl_4 and CCl_3F or radicals like CClF_2 , dissociative attachment can be dominant with respect to electron impact dissociation, as these species attach electrons almost at Langevin rates ($10^{-13} \text{ m}^3 \text{ s}^{-1}$).^{9,10} It is therefore expected that these molecules break up very efficiently under plasma conditions. For other electronegative molecules like CF_4 or SiF_4 , dissociative attachment is much slower and requires a significant

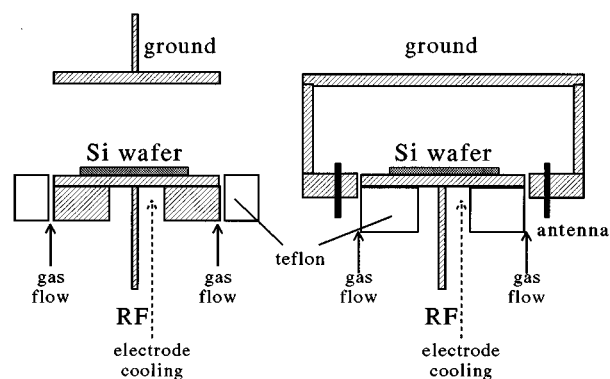


Fig. 1. A schematic view of the open and closed electrode configurations. The open configuration is used for absorption measurements, whereas the closed system is used for the electron density measurements.

threshold energy.¹¹ Therefore, these molecules are dissociated mainly by electron impact. As a result, the dissociation degrees in such plasmas are very low (less than 1% in CF_4).¹² In contrast to CF_4 , dissociative attachment to CCl_2F_2 is an exothermic process with practically no energy threshold, but it is much slower than attachment to highly chlorinated molecules. Therefore, it is not clear which of the mechanisms mentioned is important for dissociation of CCl_2F_2 . Although no data are available on the electron impact dissociation cross section, the total dissociation rate, determined from the measurements, can be used to evaluate this magnitude.

III. EXPERIMENT

A. Plasma reactor

Measurements have been carried out in a 13.56 MHz capacitively coupled plasma using two comparable geometries. The infrared spectroscopy has been performed in a parallel plate configuration with a 12.4 cm plate diameter and a variable distance between the plates (typically 5 cm). For the electron and negative ion density measurements a plasma box configuration has been used. The diameter of the powered electrode in this case is also 12.4 cm and the electrode gap is 5 cm, but the diameter of the grounded box is 17.5 cm. A scheme of the two configurations is shown in Fig. 1. In both cases the electrodes are made of aluminum. A 10 cm silicon wafer is placed on top of the lower, water cooled rf electrode in order to study the etching process. The gases are fed through mass flow controllers and introduced homogeneously through a slit around the rf electrode. The pressure in the vacuum chamber is measured using an MKS baratron. The gas pressure and flow can be varied independently from 5 to 500 mTorr and from 0 to 100 sccm, respectively, using a throttle valve in the pumping line of a turbomolecular pump. The plasma is sustained by an ENI rf generator combined with an automatic matching network to optimize the power dissipation in the discharge. The resulting input power can be varied between 0 and 120 W. The values of the rf power mentioned in Sec. IV are based on the power supplied by the

TABLE I. Total electron impact dissociation and dissociative attachment rates for various species in a CCl_2F_2 plasma.

Molecule	Total dissociation rate constant ($\text{m}^3 \text{s}^{-1}$)	Ref.	Dissociative attach. rate constant ($\text{m}^3 \text{s}^{-1}$)	Ref.
CCl_2F_2	8×10^{-15}	measured	10^{-15}	7,13
CClF_3	2×10^{-15}	measured	4×10^{-17}	14
$\text{C}_2\text{Cl}_2\text{F}_4$	$> 5 \times 10^{-15}$	measured	$2.5 \pm 0.5 \times 10^{-15}$	15
CF_4	$\approx 2 \times 10^{-16}$	measured	4×10^{-17}	16
	10^{-16}	17		
CCl_3F			10^{-13}	9
CCl_4			10^{-13}	9

rf generator. It is estimated that only about 80% is coupled into the plasma; the rest is lost in the supply lines and in the matching network.

The densities of plasma species (electrons, molecules) reproduce within 25%. This is mainly due to the history of the reactor (e.g., the presence of a deposition layer) and the irreproducibility of the matching conditions. The accuracy of the diagnostic methods described below is better than 5%. The error in the measured rate constants, given in Table I, is caused by the nonreproducibility of the plasma conditions, the error in the estimated plasma volume and the difference in the electron density between the open and closed configuration (see Fig. 1). We estimate that the absolute values of the measured rates are accurate within a factor of 2. However, the error in the relative values for the various rates is much less (about 10%).

B. Microwave resonance

In order to measure the electron density a microwave resonance method has been used in which the plasma box serves as a cavity. For this purpose a low power microwave signal of variable frequency is coupled to the plasma box by means of an antenna, thereby exciting the TM_{020} mode (frequency ~ 3 GHz). The transmission of the cavity is recorded by another antenna and processed by a digitizing oscilloscope. The resonance frequency of the cavity, which depends on the number of free electrons inside, is determined by tuning the microwave frequency to maximum transmission. From the shift of the resonance frequency with respect to its value in vacuum the average electron density in the cavity is deduced. A detailed treatment of this technique is given in Refs. 18 and 19.

C. Infrared spectroscopy

Infrared absorption spectra have been collected using a Bruker IFS-66 Fourier transform infrared spectrometer and a Laser Photonics tunable diode laser system. A scheme of the setup is shown in Fig. 2. The parallel beam exiting the Fourier transform spectrometer is directed through the reactor (single pass) on which BaF_2 windows are mounted. Afterwards the beam is focused onto a mercury cadmium telluride (MCT) photo-conductive detector, which is sensitive to wave numbers higher than 800 cm^{-1} . This means that some multiply chlorinated species (CCl_4 , SiCl_4) cannot be detected.

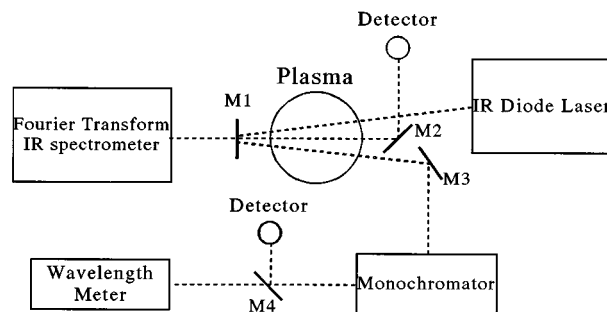


FIG. 2. Experimental setup for the infrared absorption spectroscopy with a Fourier transform infrared spectrometer and with a tunable diode laser. These systems cannot be operated simultaneously (either mirror M_1 or M_2 is installed).

Typically the spectrum is averaged over a few hundred scans to obtain a good signal to noise ratio. The spectra are collected with a wavelength resolution of 2 cm^{-1} . The densities of infrared active species have been determined using their known absorption coefficients.²⁰

The CF_2 radical density measurements have been performed by measuring CF_2 absorption in the P branch of the ν_3 band at $1096\text{--}1096.7 \text{ cm}^{-1}$ with a Laser Photonics tunable diode laser. The infrared laser beam is first directed through the plasma (double pass) and then led through a 1 m monochromator, selecting the desired laser mode. The infrared signal is detected using a MCT detector. In order to increase the signal to noise ratio a first derivative technique has been applied, in which the laser wavelength is modulated while scanning the absorption lines. This is achieved by modulating the laser current. The signal from the detector is processed using a lock-in amplifier. Absolute CF_2 densities can be determined if the absorption coefficient and the density distribution over the rotational levels are known. Details concerning the experimental technique as well as the method for the density calculation are given by Haverlag *et al.*¹² The plasma reactor is translated vertically and a 1 mm slit is placed in the laser beam in order to obtain axial CF_2 density profiles. In this case the distance between the electrodes is reduced to 3 cm.

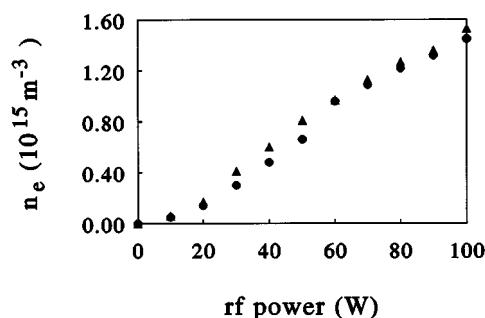


FIG. 3. Electron density as a function of rf input power in a 200 mTorr CCl_2F_2 plasma. The gas flow is 30 sccm. (●) Density with and (▲) without a silicon wafer on the rf electrode.

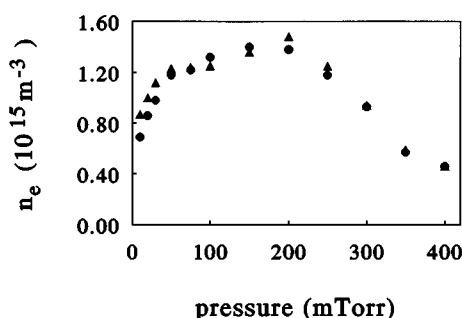


FIG. 4. Electron density as a function of pressure in a CCl_2F_2 discharge. The rf input power is 100 W and the gas flow is 30 sccm. (●) Density with and (▲) without a silicon wafer on the rf electrode.

IV. RESULTS AND DISCUSSION

A. Electron density

Since in a low pressure discharge chemically active species are formed mainly in electron induced reactions, knowledge of the electron density is essential to model the discharge chemistry. The data, obtained from microwave resonance measurements, are used to explain the dependencies of the CCl_2F_2 dissociation degree on various plasma parameters. Below we present the electron density and its dependence on rf power input, pressure, gas flow and argon admixture.

The electron density increases almost linearly with the rf power (Fig. 3). This feature has been observed for many other gases in low pressure rf discharges.¹⁸ As a function of pressure n_e reaches a maximum at about 200 mTorr (Fig. 4). Furthermore, the electron density does not vary significantly with the gas flow. Only a small increase of n_e is observed for extremely low flows (< 2 sccm).

Finally the dependence of the electron density on CCl_2F_2 admixture in an argon plasma is shown in Fig. 5. A drastic decrease in electron density is observed when even a small amount of CCl_2F_2 is added to an argon plasma. This is due to a fast loss of electrons by dissociative attachment to CCl_2F_2 . A more detailed explanation of this transition be-

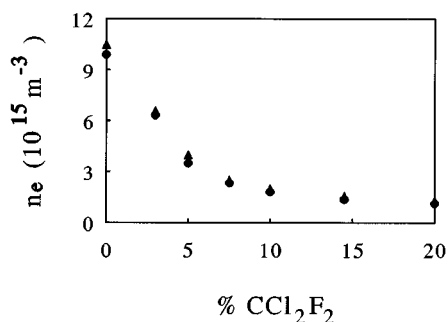


FIG. 5. Electron density in $\text{Ar}/\text{CCl}_2\text{F}_2$ mixtures as a function of the CCl_2F_2 admixture. The rf power is 50 W, the total gas flow is kept constant at 30 sccm and the pressure is 200 mTorr. The electron density does not change significantly between 20% and 100% CCl_2F_2 . (●) Density with and (▲) without a silicon wafer on the rf electrode.

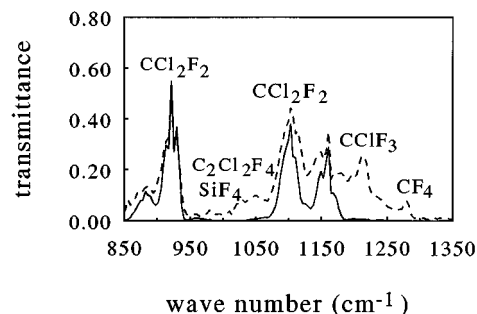


FIG. 6. Typical absorption spectra obtained with the Fourier transform infrared spectrometer. Transmittance is defined as $-\ln(I/I_0)$, where (I/I_0) is the transmission. The CCl_2F_2 gas spectrum at 200 mTorr (solid curve) is compared with the plasma spectrum at 200 mTorr and 100 W power input (5 times enlarged, dashed curve). In the plasma the CCl_2F_2 absorption is reduced, from which the dissociation degree can be determined. Note the presence of absorption bands of CF_4 at 1280 cm^{-1} , CClF_3 at 1110 and 1215 cm^{-1} and SiF_4 at 1030 cm^{-1} .

tween an electropositive and an electronegative discharge is given elsewhere.^{19,21} It should be noted that the presence of the Si wafer has only a very little influence on the electron density. A slightly lower density with Si can be attributed to poorer power coupling into the plasma due to the presence of a dielectric layer on the electrode.

B. Dissociation of CCl_2F_2

The dissociation of CCl_2F_2 and subsequent formation of other molecules have been studied by means of Fourier transform infrared spectrometry. Typical absorption spectra are given in Fig. 6. It can be seen that the fraction of CCl_2F_2 remaining in the plasma is low. As expected, fluorine rich molecules like CClF_3 , $\text{C}_2\text{Cl}_2\text{F}_4$ and CF_4 appear in significant amounts. Furthermore, in the presence of a Si wafer on the rf electrode SiF_4 absorption is detected.

Figure 7 shows the fraction of CCl_2F_2 in the plasma as a function of the gas flow at 200 mTorr and 100 W input power. Extrapolation of the flow dependence to zero flow yields a relation between dissociation and association frequencies: $\nu_{\text{ass}} \approx 0.05 \times k_{\text{dis}} n_e$. Substituting this relation into

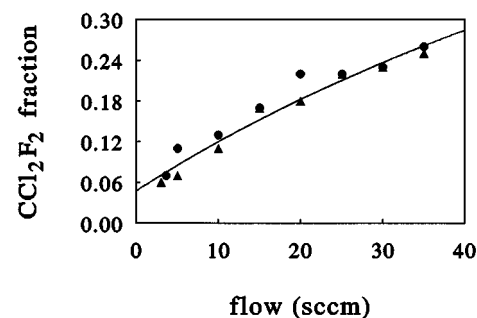


FIG. 7. Fraction of CCl_2F_2 in the plasma (ratio of partial to total pressure) as a function of CCl_2F_2 gas flow rate. The pressure is 200 mTorr and the input power is 100 W. (●) Density with and (▲) without a silicon wafer on the rf electrode. The solid curve denotes the fit to the data points obtained using Eq. (2).

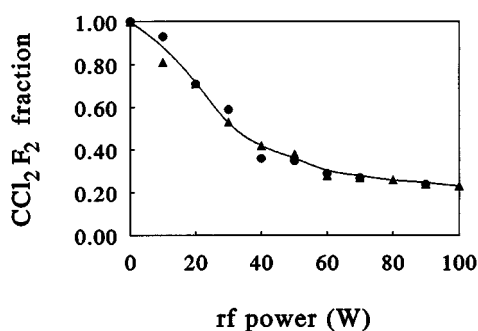


Fig. 8. Fraction of CCl_2F_2 in the plasma as a function of rf input power. The pressure is 200 mTorr and the CCl_2F_2 flow rate is 30 sccm. (●) Density with and (▲) without a silicon wafer on the rf electrode. The solid curve denotes the fit to the data points obtained using Eq. (2).

Eq. (2) and assuming that ν_{ass} is flow independent, we obtain $k_{\text{dis}}n_e = 12$ Hz, which, in combination with the experimental electron density in these conditions $n_e = 1.5 \times 10^{15} \text{ m}^{-3}$, gives $k_{\text{dis}} = 8 \times 10^{-15} \text{ m}^3 \text{ s}^{-1}$. As the dissociative attachment and ionization rates are only about $10^{-15} \text{ m}^3 \text{ s}^{-1}$, this result suggests that electron impact dissociation is the major dissociation process for CCl_2F_2 in an rf discharge.

In Fig. 8 the fraction of CCl_2F_2 left in the plasma as a function of power is shown. It can be seen that this fraction decays with increasing rf power input. This can be expected, as the electron density increases linearly with power, resulting in an increasing dissociation frequency. Introducing the experimental dependence of n_e on power together with the previously determined k_{dis} and ν_{ass} into Eq. (2), a good fit to the data points from Fig. 8 is obtained. This indicates that the dissociation process can be described well by the proposed simple model. Furthermore, as the power dependence of the dissociation degree has been fitted using a constant (power independent) dissociation rate, we conclude that there is no significant change of electron temperature with rf power.

The same procedure can be applied to the pressure dependence of the dissociation degree (see Fig. 9) using the experimental pressure dependence of the electron density from Fig. 4. However, in this case one has to account for the pressure dependent electron temperature. The latter can be

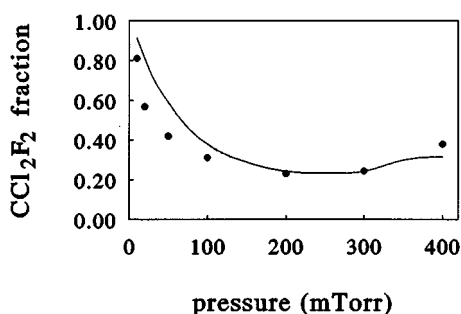


Fig. 9. Fraction of CCl_2F_2 in the plasma as a function of pressure in presence of a silicon wafer. The CCl_2F_2 flow rate is 30 sccm and the power input is 100 W. The solid curve denotes the fit to the data points obtained using Eq. (2).

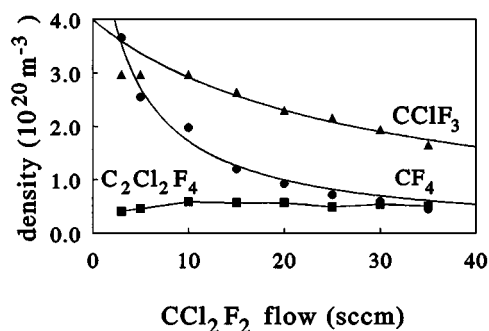


Fig. 10. Densities of reaction products in the plasma as a function of CCl_2F_2 flow rate. The pressure is 200 mTorr and the input power is 100 W; no silicon wafer is present. The CClF_3 density is fitted with $12 \times 10^{20} / (0.11 \mathcal{F} + 3)$; the CF_4 density is fitted with $2.6 \times 10^{20} / (0.11 \mathcal{F} + 0.4)$. The constant term in the denominator equals the frequency of the gas phase losses [Eq. (4)].

higher at low pressures, which results in an increased dissociation of CCl_2F_2 under these conditions. Therefore, the amount of CCl_2F_2 left in the plasma at low pressures can be lower than that predicted by the model, which neglects the temperature variations. This effect can be seen in Fig. 9.

C. Formation of stable molecules in a CCl_2F_2 discharge

From both Figs. 7 and 8 it can be seen that the presence of a Si wafer on the electrode has no significant influence on the dissociation degree of CCl_2F_2 . This conclusion, however, is not valid for products of the CCl_2F_2 conversion. In Figs. 10 and 11 the densities of various molecules are plotted as a function of gas flow in the presence and absence of a silicon wafer. The densities of halocarbon species are a factor of 2 lower in the presence of a silicon wafer on the electrode. Also, the intensities of emission lines of Cl ($\lambda = 725.7$ nm) and F ($\lambda = 685.6$ and 703.7 nm) in the presence of Si are reduced by the same factor. This suggests that Si is a sink for halogen radicals.

In a pure CCl_2F_2 discharge, without Si, the density of CF_4 decreases with the flow rate approximately as \mathcal{F}^{-1} . This molecule is formed by gas phase or surface radical as-

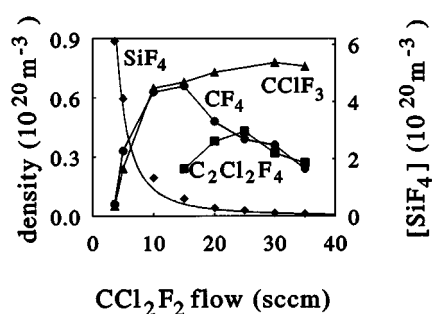


Fig. 11. Densities of reaction products in the discharge as a function of CCl_2F_2 flow rate. The pressure is 200 mTorr, input power is 100 W and a silicon wafer is placed on the rf electrode. The SiF_4 density is fitted with \mathcal{F}^{-2} .

sociation (e.g., CF₃ + F) and lost by flow and gas phase dissociation. Its density can therefore be described by

$$n = \frac{P}{\nu_{\mathcal{F}} + k_{\text{dis}}n_e} \quad (3)$$

As the radical densities are fairly flow independent (see Sec. IV D, Figs. 19 and 20), the CF₄ production P is expected to be constant with flow, at least for higher flows. Therefore, the observed flow dependence of CF₄ can be explained only if this species is flushed out of the discharge volume by the gas flow. This implies that the gas phase loss processes for CF₄ ($k_{\text{dis}}n_e$) are slower than the flow losses. The best fit to the data points shown in Fig. 10 is found for $P = 2.6 \times 10^{20} \text{ m}^{-3} \text{ s}^{-1}$ and a dissociation frequency of 0.4 Hz. Substituting our electron density gives a dissociation rate constant for CF₄ of about $2 \times 10^{-16} \text{ m}^3 \text{ s}^{-1}$, which agrees, within the experimental error, with the literature data.¹⁷

The CClF₃ density also decreases with increasing flow. As its flow dependence is much weaker than this of CF₄, a more accurate estimate can be made for the dissociation rate of this molecule. The best fit, based on Eq. (3), is obtained for a production frequency P of $1.2 \times 10^{21} \text{ m}^{-3} \text{ s}^{-1}$ and a dissociation rate k_{dis} of $2 \times 10^{-15} \text{ m}^3 \text{ s}^{-1}$. Finally, the density of the dimer (1,2-C₂Cl₂F₄) does not depend on flow, which suggests that its gas phase loss frequency is higher than 7.5 Hz ($k_{\text{dis}} > 5 \times 10^{-15} \text{ m}^3 \text{ s}^{-1}$). In analogy to CCl₂F₂, the loss rates evaluated this way can be compared with the corresponding attachment rates (see Table I). For instance, it can be seen that for CClF₃ attachment comprises only a small contribution to the total dissociation rate.

The presence of a silicon wafer not only affects the absolute molecular densities but also their dependencies on gas flow (Figs. 10 and 11). At low flow rates even the densities of stable halocarbons (CF₄) are depleted. The drastic reduction of halocarbon species at low flow rates correlates with the decrease of the halocarbon radical densities observed under these conditions (see Sec. IV D). The density of SiF₄ increases quadratically with decreasing flow. We will propose an explanation for this interesting feature, based on the production/destruction balance. As SiF₄ is a stable molecule, it is lost mainly by flow in analogy to CF₄. It has been shown that, apart from positive ions, small halogen radicals are responsible for the etching of Si.^{1,22} As the positive ion flux as well as the densities of halogen radicals are fairly constant with flow (except for extremely low flows), the etch rate is also expected to be flow independent. Therefore, if SiF₄ were formed directly at the Si surface, its production rate would be flow independent. In this case we could expect a \mathcal{F}^{-1} dependence of the SiF₄ density, similar to that of CF₄. As the observed dependence is much stronger than \mathcal{F}^{-1} , we have to conclude that SiF₄ is not the first stable product of the etching process. This first etch product, the precursor of SiF₄, can be either a stable Si containing radical, like SiF₂, or a partially chlorinated molecule. The latter is more likely, considering the composition of the reaction layer at the Si surface, which contains 15 times more Cl than F.¹ If this primary species is produced in a flow independent etching process and flushed out of the discharge volume, its density will be inversely proportional to the flow rate (like in

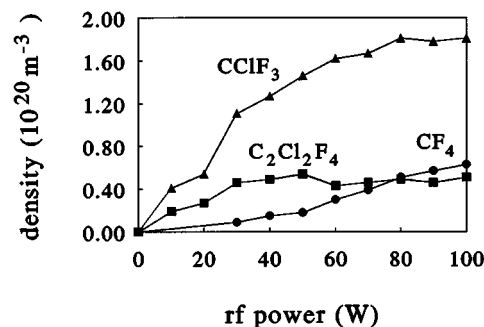


FIG. 12. Densities of reaction products in a CCl₂F₂ discharge as a function of rf input power. The pressure is 200 mTorr and the gas flow rate is 30 sccm. No silicon wafer is present.

the case of CF₄). Still, a small fraction of these molecules can react to form SiF₄. In this case the SiF₄ production rate is inversely proportional to \mathcal{F} , while its destruction rate is proportional to the flow. This yields the observed \mathcal{F}^{-2} dependence of the SiF₄ density. Estimating the etch rates provides the additional argument that SiF₄ is not the main stable etching product. The measured SiF₄ density together with the residence time in the plasma allows one to evaluate a hypothetical etch rate. The value obtained assuming that SiF₄ is the main Si containing species in the plasma does not exceed 1 Å/s. However, the etch rates determined from the heights of etch residues on the wafer surface are at least ten times higher.³ Therefore it can be concluded that SiF₄ is only a secondary etch product and, consequently, its flow dependence can be understood.

Figure 12 shows that the molecule densities increase with the rf power following the increase of the electron density (see Fig. 3). In contrast to chlorine containing molecules, the dependence of CF₄ density on power does not show saturation at high power levels. The previously analyzed flow dependence has shown that CF₄ is a stable product that is destroyed mainly by the gas flow. Its effective production rate from CCl₂F₂ must increase with increasing electron density, even though its formation involves more than one reaction step. Eventually the CF₄ density will also saturate with power if the electron density becomes high enough to induce significant gas phase losses of this molecule. The chlorinated molecules are produced in a way similar to CF₄ and therefore their production rates should also increase with increasing power input. However, these molecules are less stable in the gas phase than CF₄ and therefore they are at least partly destroyed by electron induced dissociation. The frequency of the latter process is also proportional to the electron density. This explains the saturation of the chlorinated species densities at high power levels. Note that, if a given molecule is destroyed mainly by electron impact (C₂Cl₂F₄), its density is fairly independent of the power input.

The power dependence of the molecule densities in presence of a Si wafer, shown in Fig. 13, resembles the one shown in Fig. 12. Only at higher input powers halocarbon densities tend to decrease as SiF₄ emerges. This effect is stronger in CCl₂F₂ mixtures with Ar. In Fig. 14 the power

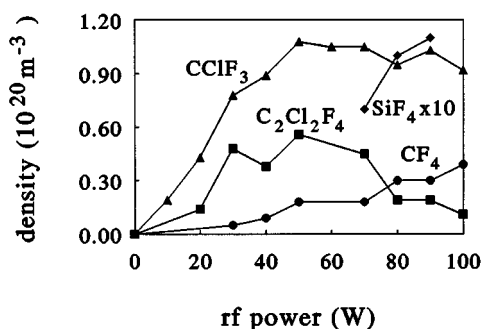


FIG. 13. Densities of reaction products in a CCl_2F_2 discharge as a function of rf input power. The pressure is 200 mTorr, the gas flow rate is 30 sccm and a silicon wafer is placed on the rf electrode.

dependencies of molecule densities are shown in an etching mixture containing 10% CCl_2F_2 in Ar. The density of SiF_4 increases linearly with power input.

The behavior of various molecular densities in Ar/ CCl_2F_2 etching mixtures is shown in Fig. 15. The fraction of CCl_2F_2 remaining in the plasma decreases significantly for large argon admixtures. This can be expected, as the electron density is higher under these conditions (see Fig. 5). The peak of the SiF_4 density at low partial pressures of CCl_2F_2 reflects an increased etch rate in Ar/ CCl_2F_2 mixtures. These are also the conditions under which cluster formation from the etch products occurs.^{2,3} It is known that positive ion flux to the substrate increases with a decreasing partial pressure of halocarbon.^{19,21} If we assume that, in the etching process both radicals and positive ions are involved, the maximum in the etch rate at low CCl_2F_2 fractions can be understood as a compromise between the increasing ion flux and the decreasing halogen radical densities. The increased etch rate and, consequently, the increased density of Si containing species correlate with a depletion of the halogen radicals, which in turn lowers the density of halocarbon molecules. This effect can be seen for the CClF_3 density in Fig. 15.

D. CF_2 densities

CF_2 is relatively stable and therefore it is expected to be one of the most abundant halocarbon radicals in our dis-

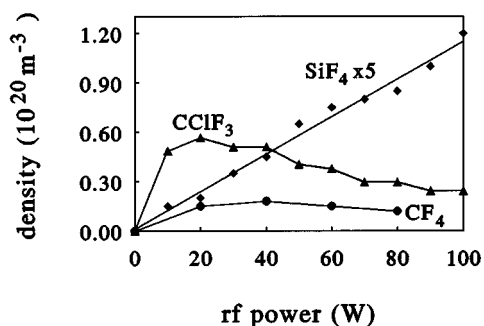


FIG. 14. Densities of CF_4 , CClF_3 and SiF_4 as a function of the rf power input in a discharge containing 10% CCl_2F_2 in argon. The pressure is 200 mTorr and the total gas flow rate is 30 sccm.

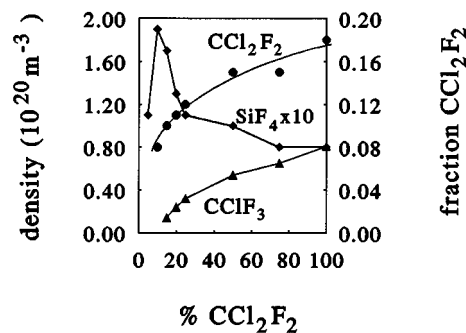


FIG. 15. Fraction of CCl_2F_2 remaining in the plasma and densities of reaction products in an Ar/ CCl_2F_2 discharge as a function of CCl_2F_2 partial pressure. The total pressure is 200 mTorr, the rf input power is 100 W and the total (Ar + CCl_2F_2) gas flow rate is 30 sccm. A silicon wafer is placed on the rf electrode.

charge. Its density has been measured for various discharge conditions by absorption spectroscopy using a tunable diode laser. The axial profiles of the CF_2 density are shown in Fig. 16. The peculiar increase of this density towards the wall indicates that CF_2 is formed mainly at the electrodes. This occurs when the less stable radicals, like, CClF_2 , convert at the wall to a more stable CF_2 , which then diffuses into the discharge. A more detailed treatment of this effect, which has been observed in many halocarbon discharges, is given by Haverlag *et al.*¹² An interesting conclusion following from the density profile in Fig. 16 is that CF_2 is actually *destroyed* in the plasma. Destruction by electron impact dissociation or attachment is unlikely due to a high dissociation energy for a C–F bond and an inert electronic configuration of this radical. A possible destruction mechanism for CF_2 is recombination with other radicals, e.g., Cl and F. Even though these reactions are three body processes, they are fast enough ($10^{-39} \text{ m}^6 \text{ s}^{-1}$ for $\text{CF}_3 + \text{F}$ and $10^{-41} \text{ m}^6 \text{ s}^{-1}$ for $\text{CF}_2 + \text{F}$)²³ to contribute significantly to the destruction of halocarbon radicals. Figure 17 shows that the CF_2 density is practically independent of the applied rf power, except for the low power regime. Similar dependencies have also been observed for some chlorinated stable molecules like

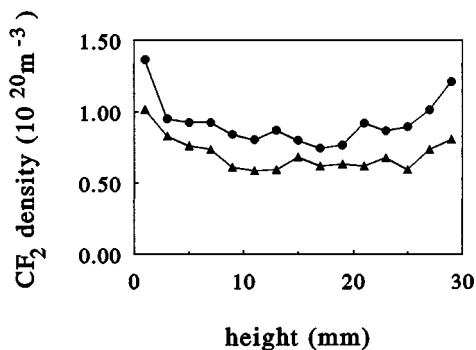


FIG. 16. Axial profile of the CF_2 radical density in a CCl_2F_2 discharge. The pressure is 200 mTorr, the rf input power is 100 W and the gas flow rate is 30 sccm. The rf electrode is at 0 mm and the grounded electrode is at 30 mm. (●) Density with and (▲) without a silicon wafer on the rf electrode. In both cases the densities increase towards the electrodes.

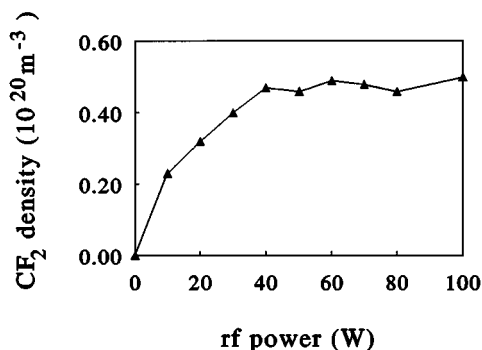


FIG. 17. CF_2 radical density in a CCl_2F_2 discharge as a function of rf power (no Si wafer). The measurements have been performed 2 cm above the rf electrode, with an electrode distance of 5 cm. The pressure is 65 mTorr and the gas flow rate is 30 sccm.

$\text{C}_2\text{Cl}_2\text{F}_4$ (see Fig. 12). This kind of behavior is expected for molecules and radicals, which are produced and destroyed by similar processes. CF_2 is clearly an intermediate product of radical reactions. It is produced from other radicals at the wall and possibly also in the discharge, and destroyed again by radical recombination. Consequently, the CF_2 density is expected to be only weakly dependent on plasma parameters. Indeed, from Figs. 18 and 19 it follows that the CF_2 density does not change much with pressure and flow rate. However, it is interesting to study the difference in the behavior of the CF_2 density as a function of flow with and without a silicon wafer on the rf electrode. In the presence of a silicon wafer the CF_2 density at high flow rates is higher than in a pure plasma without a wafer. This implies that, at higher flows, either the CF_2 production is increased due to a more efficient conversion at the silicon surface (e.g., $\text{CF}_2\text{Cl} + \text{Si} \rightarrow \text{CF}_2 + \text{SiCl}$) or the destruction is reduced, which can be due to a lower density of halogen radicals in the presence of Si. The latter seems very likely, as the emission intensities of Cl and F are a factor of 2 lower in the presence of Si (see Fig. 20). This is due to an enhanced loss of halogen radicals at the Si surface. At low flow rates a significant depletion of the CF_2 and halogen density is observed (Figs. 19 and 20). Under these conditions the source gas and the halocarbon molecule

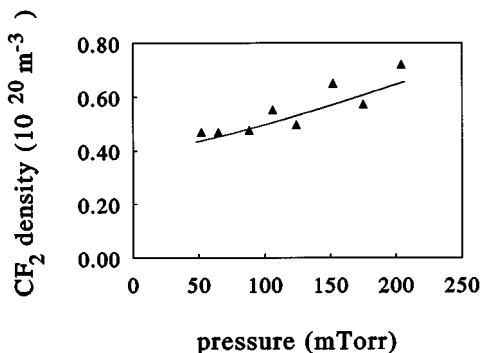


FIG. 18. CF_2 radical density in a CCl_2F_2 discharge as a function of pressure (no Si wafer). The measurements have been performed 2 cm above the rf electrode, with an electrode distance of 5 cm. The rf input power is 100 W and the gas flow rate is 30 sccm.

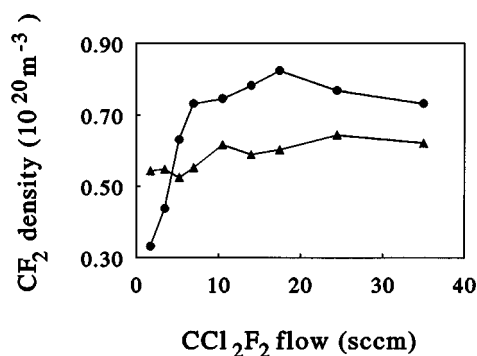


FIG. 19. CF_2 radical density in a CCl_2F_2 discharge as a function of the gas flow rate. The measurements have been performed 1.5 cm above the rf electrode, with an electrode distance of 3 cm. The rf input power is 100 W and the pressure is 200 mTorr. (●) Density with and (▲) without a silicon wafer on the rf electrode.

densities are also depleted (see Figs. 7 and 11) and converted into halosilicides (see Fig. 11). As the loss rate of the radicals at the surface is not expected to be strongly flow dependent, the negative correlation between the radical densities and the SiF_4 density as a function of flow suggests a gas phase loss process of both halocarbon and halogen radicals with Si.

A similar effect can be seen in Fig. 21, where the CF_2 density as a function of CCl_2F_2 admixture in argon is shown with and without a silicon wafer. Without a wafer the density is fairly constant except for very small admixtures. In the presence of a wafer the density is higher for large admixtures but decreases much faster with increasing argon density. This is consistent with the previously discussed flow dependence (Fig. 19), since the SiF_4 density increases with decreasing CCl_2F_2 partial pressure (until it reaches a maximum at 10% CCl_2F_2). Consequently, the radical and halocarbon molecule densities are strongly depleted at low CCl_2F_2 partial pressures in the presence of a Si wafer (Figs. 15 and 21).

V. CONCLUSIONS

The plasma chemistry of CCl_2F_2 has been studied in a pure CCl_2F_2 discharge and in CCl_2F_2 mixtures with argon. These mixtures attract special attention due to their enhanced etching capacity. Electron impact dissociation, dissociative attachment and ionization reactions drive most of the chemi-

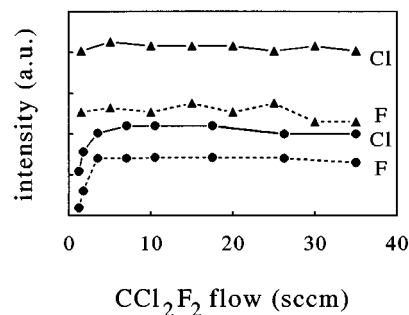


FIG. 20. Emission intensities of Cl ($\lambda = 725.7$ nm) and F ($\lambda = 703.7$ nm) as a function of the gas flow. The intensities are denoted by (●) (in presence of Si) or (▲) (without Si).

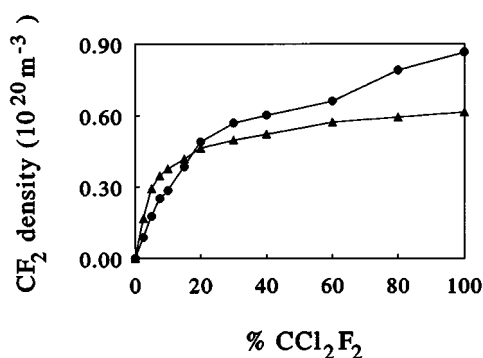


FIG. 21. CF_2 radical density in an $\text{Ar}/\text{CCl}_2\text{F}_2$ discharge as a function of the CCl_2F_2 admixture. The measurements have been performed 1.5 cm above the rf electrode, with an electrode distance of 3 cm. The rf input power is 100 W, the pressure is 200 mTorr and the total gas flow rate is 30 sccm. (●) Density with and (▲) without a silicon wafer on the rf electrode.

cal processes in these plasmas, which makes the electron density a very essential plasma parameter. The electron density is proportional to the input power; it does not vary with gas flow and it is weakly dependent on pressure. In most cases a large fraction of the source gas is dissociated and a wide variety of new species is formed. The fluorine rich halocarbons, in particular, are readily formed due to their thermodynamical stability. From the dependence of molecular densities on gas flow rates the total dissociation rate of several molecules can be deduced (Table I). In the presence of a silicon wafer the chemistry is strongly affected, as the silicon consumes halogen radicals. This may enhance or decrease the densities of a particular species depending on whether this species is produced from or destroyed by the halogens. All measurements performed with a Si wafer show a negative correlation between the density of the etch product SiF_4 and the halogen radical or halocarbon molecule densities, such as Cl, F and CClF_3 . Moreover, at very low flow rates and in the presence of Si even the CF_2 density decreases. From the dependence of the SiF_4 density on the flow

rate it can be concluded that SiF_4 is not the primary etch product, but it is formed from other Si containing species that are released from the surface.

- ¹Y. Zhang, G. S. Oehrlein, E. De Fresart, and J. W. Corbett, *J. Appl. Phys.* **71**, 1936 (1992).
- ²(a) G. S. Selwyn, *J. Vac. Sci. Technol. B* **9**, 3487 (1991); (b) G. S. Selwyn and E. F. Patterson, *J. Vac. Sci. Technol. A* **10**, 1053 (1992).
- ³W. W. Stoffels, E. Stoffels, G. M. W. Kroesen, M. Haverlag, J. H. W. G. den Boer, and F. J. de Hoog, *Plasma Sources Sci. Technol.* **3**, 320 (1994).
- ⁴T. Kaneda, T. Kubota, M. Ohuchi, and J.-S. Chang, *J. Phys. D* **23**, 1642 (1990).
- ⁵E. Stoffels, W. W. Stoffels, L. C. T. Verhamme, E. Van Wieringen, G. M. W. Kroesen, and F. J. de Hoog, *Europhysics Conference Abstracts Vol. 16 F, Proceedings of ESCAMPIG XI*, 455, St. Petersburg, Russia, 25–28 August 1992 (European Physical Society, St. Petersburg, 1992).
- ⁶J. A. O'Neill, J. Singh, and G. G. Gifford, *J. Vac. Sci. Technol. A* **8**, 1716 (1990).
- ⁷V. M. Pejcev, M. V. Kurepa, and I. M. Cadez, *Chem. Phys. Lett.* **63**, 301 (1979).
- ⁸A. T. Bell, *Ind. Eng. Chem. Fundam.* **10**, 373 (1971).
- ⁹D. Smith, N. G. Adams, and E. Alge, *J. Phys. B: At. Mol. Phys.* **17**, 461 (1984).
- ¹⁰N. G. Adams, D. Smith, and C. R. Herd, *Int. J. Mass Spectrom. Ion Processes* **84**, 243 (1988).
- ¹¹I. Iga, M. V. V. S. Rao, S. K. Srivastava, and J. C. Nogueira, *Z. Phys. D: At. Mol. Clusters* **24**, 111 (1992).
- ¹²M. Haverlag, E. Stoffels, W. W. Stoffels, G. M. W. Kroesen, and F. J. de Hoog, *J. Vac. Sci. Technol. A* **12**, 3102 (1994).
- ¹³D. L. McCorkle, A. A. Christodoulides, L. G. Christophorou, and I. Szamrej, *J. Chem. Phys.* **72**, 4049 (1980); for CCl_3F , see also *J. Chem. Phys.* **76**, 753 (1982).
- ¹⁴S. M. Spyrou and L. G. Christophorou, *J. Chem. Phys.* **82**, 2620 (1985).
- ¹⁵D. L. McCorkle, I. Szamrej, and L. G. Christophorou, *J. Chem. Phys.* **77**, 5542 (1982).
- ¹⁶S. R. Hunter, J. G. Carter, and L. G. Christophorou, *Phys. Rev. A* **38**, 58 (1988).
- ¹⁷D. Edelson and D. L. Flamm, *J. Appl. Phys.* **56**, 1522 (1984).
- ¹⁸M. Haverlag, A. Kono, D. Passchier, G. M. W. Kroesen, W. J. Goedheer, and F. J. de Hoog, *Appl. Phys.* **70**, 3472 (1991).
- ¹⁹E. Stoffels, W. W. Stoffels, D. Vender, G. M. W. Kroesen, and F. J. de Hoog, *J. Vac. Sci. Technol. A* **13**, 2049 (1995).
- ²⁰*Matheson Gas Data Book*, 6th ed., edited by W. Braker and A. L. Mossman (Matheson Gas, Lyndhurst, NJ, 1980).
- ²¹E. Stoffels, W. W. Stoffels, D. Vender, G. M. W. Kroesen, and F. J. de Hoog, *Proceedings of the 11th International Symposium on Plasma Chemistry Loughborough, UK, 1993* (unpublished), Vol. 4, p. 1587.
- ²²J. W. Coburn, *J. Vac. Sci. Technol. A* **12**, 617 (1994).
- ²³I. C. Plumb and K. R. Ryan, *Plasma Chem. Plasma Proc.* **6**, 11 (1986).